

Superconductivity and crystalline electric field effects in the filled skutterudite series $\text{Pr}(\text{Os}_{1-x}\text{Ru}_x)_4\text{Sb}_{12}$

N. A. Frederick, T. D. Do, P.-C. Ho, N. P. Butch, V. S. Zapf, and M. B. Maple

Department of Physics and Institute for Pure and Applied Physical Sciences, University of California at San Diego, La Jolla, California 92093-0350, USA

(Received 1 July 2003; published 30 January 2004)

X-ray powder-diffraction, magnetic-susceptibility $\chi(T)$, and electrical resistivity $\rho(T)$ measurements were made on single crystals of the filled skutterudite series $\text{Pr}(\text{Os}_{1-x}\text{Ru}_x)_4\text{Sb}_{12}$. One end of the series ($x=0$) is a heavy fermion superconductor with a superconducting critical temperature $T_c=1.85$ K, while the other end ($x=1$) is a conventional superconductor with $T_c\approx 1$ K. The lattice constant a decreases approximately linearly with increasing Ru concentration x . As Ru (Os) is substituted for Os (Ru), T_c decreases nearly linearly with substituent concentration and exhibits a minimum with a value of $T_c=0.75$ K at $x=0.6$, suggesting that the two types of superconductivity compete with one another. Crystalline electric field effects in $\chi_{\text{dc}}(T)$ and $\rho(T)$ due to the splitting of the Pr^{3+} ninefold degenerate Hund's rule $J=4$ multiplet are observed throughout the series, with the splitting between the ground state and the first excited state increasing monotonically as x increases. The fits to the $\chi_{\text{dc}}(T)$ and $\rho(T)$ data are consistent with a Γ_3 doublet ground state for all values of x , although reasonable fits can be obtained for a Γ_1 ground state for x values near the end member compounds ($x=0$ or $x=1$).

DOI: 10.1103/PhysRevB.69.024523

PACS number(s): 74.25.Fy, 74.25.Ha, 74.62.Dh, 71.27.+a

I. INTRODUCTION

The filled skutterudite compound $\text{PrOs}_4\text{Sb}_{12}$ was recently discovered to be the first Pr-based heavy fermion superconductor, with a superconducting transition temperature $T_c=1.85$ K and an effective mass $m^*\approx 50m_e$, where m_e is the free-electron mass.^{1,2} Features in the dc magnetic susceptibility $\chi_{\text{dc}}(T)$, specific heat $C(T)$, electrical resistivity $\rho(T)$, and inelastic neutron scattering (INS) can be associated with the thermally dependent population of the ninefold degenerate $\text{Pr}^{3+}J=4$ Hund's rule multiplet split by a cubic crystalline electric field (CEF). These data suggest that the ground state of $\text{PrOs}_4\text{Sb}_{12}$ is a Γ_3 doublet, separated from a Γ_5 triplet first excited state by ~ 10 K.^{1,2} The possibility of a Γ_1 singlet ground state has also been put forward based on other measurements,^{3,4} some of which also consider tetrahedral symmetry operators in their calculations of the CEF Hamiltonian of $\text{PrOs}_4\text{Sb}_{12}$.⁵ It has been proposed that the superconductivity in $\text{PrOs}_4\text{Sb}_{12}$ may be due to quadrupolar fluctuations,¹ a claim that has been supported by muon spin resonance⁶ (μSR) and Sb-nuclear quadrupole resonance⁷ (Sb-NQR) measurements, which indicate a strong-coupling isotropic energy gap of $2\Delta\approx 5k_B T_c$. Other intriguing effects are seen in $\text{PrOs}_4\text{Sb}_{12}$, including multiple superconducting transitions⁸⁻¹⁰ and phases,¹¹ and an ordered phase that is observed in high magnetic fields and at low temperatures.¹² This high-field ordered phase (HFOP), which is seen in measurements of $\rho(T)$,¹² $C(T)$,^{3,9} magnetization $M(T)$,¹³ and thermal expansion $\alpha(T)$ (Ref. 10) in a magnetic field H , as well as measurements of $\rho(H)$ (Ref. 13) and magnetostriction $\lambda(H)$ (Ref. 14) isotherms, appears to be related to the crossing of the CEF energy levels in magnetic fields.^{9,15} In addition, neutron-diffraction experiments⁴ indicate the presence of quadrupolar effects in the HFOP, analogous to those seen in PrPb_3 .¹⁶ $\text{PrOs}_4\text{Sb}_{12}$ has proven to be a unique com-

pound, and will continue to provide a fertile area of research for many years.

The isostructural compound $\text{PrRu}_4\text{Sb}_{12}$ displays superconductivity below $T_c\approx 1.0$ K and possesses an electronic specific-heat coefficient γ approximately five to ten times smaller than $\text{PrOs}_4\text{Sb}_{12}$, identifying it as a conventional metal or at most a borderline heavy fermion metal.¹⁷ It was previously reported, based on measurements of $\chi_{\text{dc}}(T)$, to possess a Γ_1 ground state and a Γ_4 triplet first excited state ≈ 70 K above the ground state.¹⁷ A later measurement of $\rho(T)$ also supported this CEF level scheme.¹⁸ $\text{PrRu}_4\text{Sb}_{12}$ appears to be a BCS-like weak-coupling superconductor, with an isotropic s -wave energy gap of $2\Delta\approx 3k_B T_c$, as determined from Sb-NQR measurements.¹⁹ At the present time, no quadrupolar effects or features resembling the HFOP seen in $\text{PrOs}_4\text{Sb}_{12}$ have been reported in $\text{PrRu}_4\text{Sb}_{12}$.

The substitution of $\text{PrRu}_4\text{Sb}_{12}$ into $\text{PrOs}_4\text{Sb}_{12}$ to form $\text{Pr}(\text{Os}_{1-x}\text{Ru}_x)_4\text{Sb}_{12}$ was undertaken to investigate the evolution of the superconductivity, the CEF energy-level scheme, and the heavy fermion state with Ru doping, and to investigate the relationship, if any, between these three phenomena. The present study focuses on measurements of $\chi(x,T)$ and $\rho(x,T)$, which have revealed the x dependencies of T_c and the splitting between the CEF ground state and the first excited state. We are also in the process of investigating the heavy fermion state via measurements of $C(T)$ and the upper critical field $H_{c2}(T)$ through measurements of $\rho(T,H)$ (which will also reveal the x dependence of the HFOP), and will report these results in a future publication.

II. EXPERIMENTAL DETAILS

Single crystals of $\text{Pr}(\text{Os}_{1-x}\text{Ru}_x)_4\text{Sb}_{12}$ were grown using an Sb flux method. The elements (Ames 99.999% Pr, Colonial Metals 99.95% Os and 99.9% Ru, and Alfa Aesar

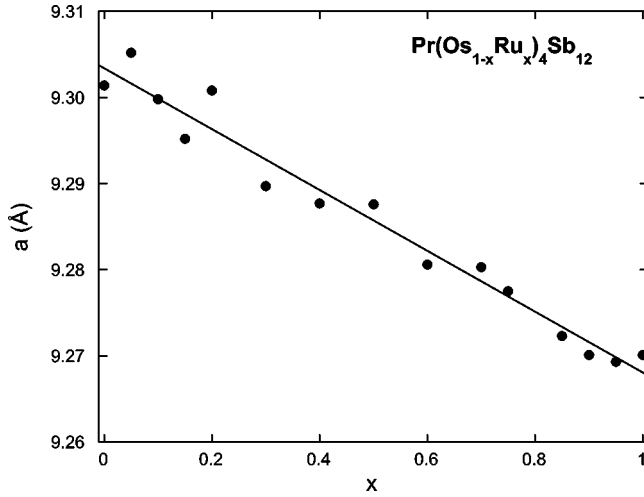


FIG. 1. Lattice parameter a as a function of Ru concentration x . The solid line is a linear least-squares fit to a vs x .

99.9999% Sb) were sealed under 150 Torr Ar in a carbon-coated quartz tube in the ratio 1:4–4 x :4 x :20, heated to 1050 °C at 50 °C/h, then cooled at 2 °C/h to 700 °C. The samples were then removed from the furnace and the excess Sb was spun off in a centrifuge. The crystals were removed from the leftover flux by etching with dilute aqua regia (HCl:HNO₃:H₂O = 1:1:3).

X-ray powder-diffraction measurements were made at room temperature using a Rigaku D/MAX B x-ray machine. The only significant impurities in any of the samples were identified with free Sb that was still attached to the crystals. Each Pr(Os_{1-x}Ru_x)₄Sb₁₂ sample crystallized in the LaFe₄P₁₂ structure²⁰ with a lattice constant a that decreased roughly linearly with increasing Ru concentration x , as displayed in Fig. 1. A silicon standard was used in order to achieve a more accurate determination of the lattice constant. Measurements of χ_{dc} vs temperature T were made in a magnetic field H of 0.5 T between 1.8 and 300 K in a commercial Quantum Design superconducting quantum interference device magnetometer. Measurements of ρ and χ_{ac} were made as a function of T down to 1.2 K in a ⁴He cryostat and, for several of the samples, down to 0.1 K in a ³He-⁴He dilution refrigerator. Many of the crystals used to measure ρ were small and irregularly shaped, which introduces an uncertainty in the geometrical factor used to convert resistance to ρ .

III. RESULTS

A. Magnetic susceptibility

Displayed in the main portion of Fig. 2 is a plot of the dc magnetic susceptibility χ_{dc} as a function of temperature T for single crystals of Pr(Os_{1-x}Ru_x)₄Sb₁₂ with various values of x . Above $T \approx 100$ K, the inverse magnetic susceptibility $1/\chi_{dc}$ is linear, indicating Curie-Weiss behavior. The data have been corrected for excess Sb by assuming that the high-temperature effective moment μ_{eff} of Pr should be equal to the Hund's rule free ion value of $3.58\mu_B$ for Pr³⁺, where μ_B is the Bohr magneton. Any deviation from this value was attributed to free Sb inclusions in the Pr(Os_{1-x}Ru_x)₄Sb₁₂

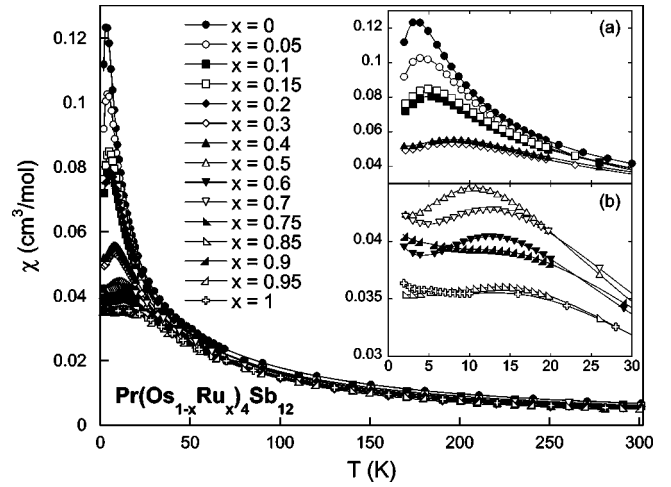


FIG. 2. dc magnetic susceptibility χ_{dc} as a function of temperature T between 1.8 and 300 K for single crystals of Pr(Os_{1-x}Ru_x)₄Sb₁₂. Inset (a) χ_{dc} vs T between 1.8 and 30 K, showing the evolution of the peak due to crystalline electric field effects for the Ru concentrations $x=0$ – $x=0.4$. The $x=0.2$ sample has been removed for clarity. Inset (b) as inset (a), but for Ru concentrations $x=0.5$ – $x=1$. The samples with $x=0.75$ and $x=0.95$ were removed for clarity.

crystals. The most significant effect on χ_{dc} from this correction was not the small diamagnetic Sb signal but instead the change in overall scaling due to the difference in mass used to calculate χ_{dc} in units of cm³/mol from the raw magnetization data. The calculated percentages of mass attributed to Sb out of the total sample volume for all values of x are listed in Table I. The estimated value of the Sb mass depends slightly on the CEF ground state used to make the fit correction; only the values for a Γ_3 ground state are given for simplicity.

All of the Pr(Os_{1-x}Ru_x)₄Sb₁₂ samples exhibit features (peaks or plateaus) in χ_{dc} that can be attributed to CEF effects. These features are the focus of the two insets in Fig. 2. The low-temperature χ_{dc} data for the samples from $x=0$ to $x=0.4$ are shown in Fig. 2(a), while Fig. 2(b) similarly displays data for the samples from $x=0.5$ to $x=1$. An explanation of the fits used to determine the CEF parameters from the χ_{dc} data, as well as the parameters themselves, are given in Sec. IV B.

Low-temperature (<2 K) ac magnetic susceptibility χ_{ac} vs T data for Pr(Os_{1-x}Ru_x)₄Sb₁₂ are shown in Fig. 3. A sharp diamagnetic transition can be seen for all values of x , indicating the presence of superconductivity. The superconducting critical temperature T_c for each concentration was determined from the data displayed in Fig. 3 as the midpoint of the diamagnetic transition. A plot of T_c vs x is displayed in Fig. 6, and is discussed further in Sec. IV A. An additional feature of note is the steplike structure that appears in the χ_{ac} data for PrOs₄Sb₁₂. Since double superconducting transitions have been observed in specific-heat and thermal-expansion measurements on both collections of single crystals and individual single crystals,^{8–10} it is reasonable to assume that this step in the diamagnetic transition for PrOs₄Sb₁₂ is also due to an intrinsic second superconducting

TABLE I. Physical properties of $\text{Pr}(\text{Os}_{1-x}\text{Ru}_x)_4\text{Sb}_{12}$ compounds. x is the concentration of Ru; $\rho(300\text{ K})$ is the electrical resistivity ρ at 300 K; $\rho(0\text{ K})$ is ρ at 0 K extrapolated from CEF fits (see text); RRR is the residual resistivity ratio, defined as $\rho(300\text{ K})/\rho(0\text{ K})$; %Sb is the percentage of the mass attributed to free Sb in $\chi_{\text{dc}}(T)$ assuming a Γ_3 ground state; x_{LLW} and W are the Lea, Leask, and Wolf parameters;³⁰ and ΔE_{a-b} is the energy difference between the ground state Γ_a and the first excited state Γ_b .

x	$\rho(300\text{ K})$ ($\mu\Omega\text{ cm}$)	$\rho(0\text{ K})$ ($\mu\Omega\text{ cm}$)	RRR	%Sb	x_{LLW} Γ_3 ground state	W	ΔE_{3-5} (K)	x_{LLW} Γ_1 ground state	W	ΔE_{1-5} (K)	ΔE_{1-4} (K)
0	155	1.67	93	25.0	-0.721	-5.69	10.1	0.500	1.99	5.87	
0.05	235	18.7	13	15.1	-0.720	-6.38	12.1	0.484	1.47	7.08	
0.1	259	46.0	5.6	21.3	-0.717	-7.05	15.9	0.462	1.31	9.54	
0.15	215	27.0	8.0	15.6	-0.718	-7.00	14.9	0.452	1.11	9.43	
0.2	510	54.0	9.4	27.3	-0.713	-6.16	16.6				
0.3				8.0	-0.707	-7.48	25.5				
0.4	343	58.2	5.9	20.2	-0.702	-6.43	25.2				
0.5				4.9	-0.687	-6.06	34.2				
0.6	305	67.4	4.5	6.6	-0.675	-5.75	40.3				
0.7	166	34.8	4.8	10.1	-0.663	-4.81	40.4				
0.75				17.2	-0.669	-5.54	42.8				
0.85				6.3	-0.670	-6.05	46.4	-0.737	2.70		87.4
0.9	330	42.4	7.8	11.9	-0.646	-4.58	47.7	-0.872	3.43		78.8
0.95				20.8	-0.665	-5.94	48.8	-0.970	5.51		88.7
1	578	41.8	14	7.4	-0.655	-5.45	50.8	-0.946	4.95		88.1

phase instead of a variation of T_c throughout the multiple crystals used in the χ_{ac} measurements. None of the other concentrations display significant structure in their superconducting transitions, although the transitions for $x=0.3$ and $x=0.4$ are much wider than for the other concentrations. This may be due to a variation of T_c between individual crystals for these two concentrations.

B. Electrical resistivity

The main portion of Fig. 4 displays high-temperature electrical resistivity ρ vs T data for $\text{Pr}(\text{Os}_{1-x}\text{Ru}_x)_4\text{Sb}_{12}$ for

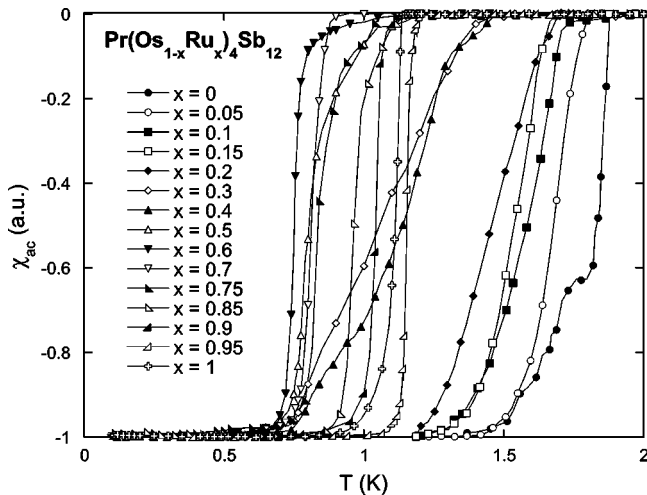


FIG. 3. ac magnetic susceptibility χ_{ac} as a function of temperature T between 0.1 and 2 K for single crystals of $\text{Pr}(\text{Os}_{1-x}\text{Ru}_x)_4\text{Sb}_{12}$. The data have been normalized to 0 at $T = 2\text{ K}$ and to -1 at $T = 0\text{ K}$ for clarity.

various values of x between 0 and 1. The extrapolated values of ρ at zero temperature taken from fits to the $\rho(T)$ data based on calculations of $\rho(T)$ that incorporate CEF splitting of the Pr^{3+} $J=4$ multiplet (see Sec. IV B), $\rho(0\text{ K})$, are plotted vs x in the inset to Fig. 4. These $\rho(0\text{ K})$ values, as well as the values of ρ at room temperature, $\rho(300\text{ K})$, and the residual resistivity ratio (RRR), defined as $\rho(300\text{ K})/\rho(0\text{ K})$, are listed in Table I. It is surprising that the RRR of $\text{PrRu}_4\text{Sb}_{12}$ is so much lower than that of

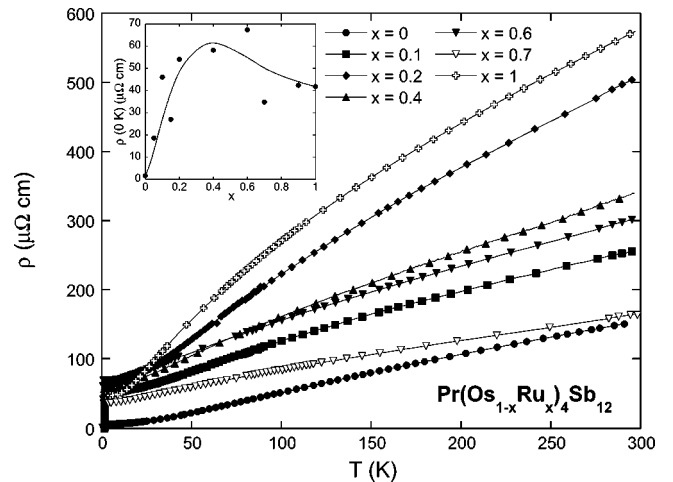


FIG. 4. Electrical resistivity ρ as a function of temperature T between 0.4 and 300 K for single crystals of $\text{Pr}(\text{Os}_{1-x}\text{Ru}_x)_4\text{Sb}_{12}$ with various values of x between 0 and 1. The samples with $x = 0.05$, $x = 0.15$, and $x = 0.9$ were removed for clarity. Inset: extrapolated values of ρ at zero temperature from fits to the $\rho(T)$ data based on CEF splitting considerations (see text for details), $\rho(0\text{ K})$ vs x . The solid line is a guide to the eye.

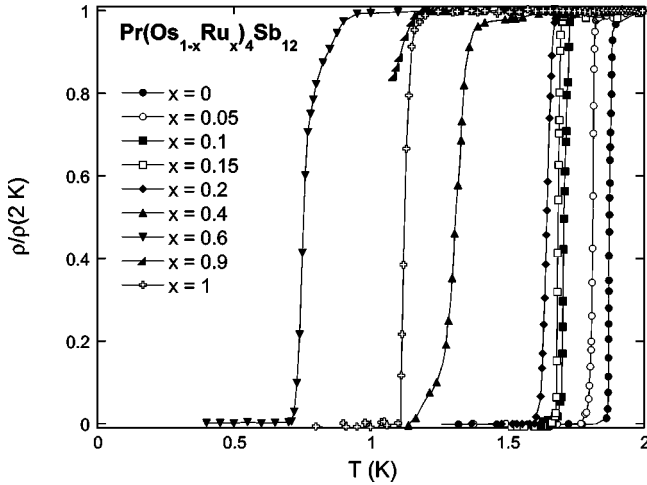


FIG. 5. Electrical resistivity ρ as a function of temperature T between 0.4 and 2 K for single crystals of $\text{Pr}(\text{Os}_{1-x}\text{Ru}_x)_4\text{Sb}_{12}$ with various values of x between 0 and 1, normalized to their values at 2 K. The data for the sample with $x=0.7$ are not shown because it did not superconduct down to the lowest temperature measured (see text for details). Similarly, the superconducting transition for $x=0.9$ is not complete due to the low-temperature limit of the measurement of this sample.

$\text{PrOs}_4\text{Sb}_{12}$, since they are both stoichiometric compounds and would be expected to have a low residual resistivity. A previous measurement of $\text{PrRu}_4\text{Sb}_{12}$ found $\rho(300\text{ K}) = 632\ \mu\Omega\text{ cm}$ and a RRR of 25,¹⁷ in reasonable agreement with the data presented in this paper. The low RRR of $\text{PrRu}_4\text{Sb}_{12}$ is not presently understood.

The electrical resistivity of $\text{Pr}(\text{Os}_{1-x}\text{Ru}_x)_4\text{Sb}_{12}$ below $T = 2\text{ K}$ is shown in Fig. 5. The data have been normalized to their values at 2 K in order to emphasize the superconducting transitions. The $x=0.7$ sample did not display the onset of superconductivity down to the lowest measured temperatures and no data for this sample are shown in this plot; the heating due to large contact resistances in the $x=0.7$ and $x=0.9$ samples precluded measurements below 1 K. The superconducting transitions as determined from $\rho(T)$ are in reasonable agreement with those measured inductively (Fig. 3), and the plot of T_c vs x is discussed in the following section.

IV. ANALYSIS AND DISCUSSION

A. Superconductivity

The dependence of the superconducting transition temperature T_c on Ru concentration x for $\text{Pr}(\text{Os}_{1-x}\text{Ru}_x)_4\text{Sb}_{12}$ is shown in Fig. 6. Several concentrations have more than one data point associated with them, which are from measurements of different crystals. These additional measurements were not shown in Figs. 4 and 5 or listed in Table I in the interest of clarity. The RRR's were nearly identical for all crystals of a given concentration, with the exception of the $x=0.2$ samples where the crystal with the lowest T_c in Fig. 6 had an RRR about half of that measured for the other two $x=0.2$ samples, one of which is listed in Table I. The vertical

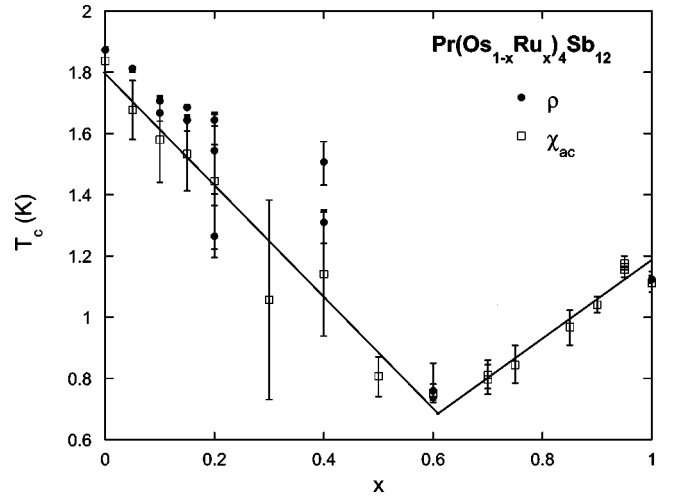


FIG. 6. Superconducting critical temperature T_c vs Ru concentration x for $\text{Pr}(\text{Os}_{1-x}\text{Ru}_x)_4\text{Sb}_{12}$. Filled circles: T_c extracted from electrical resistivity ρ . Open squares: T_c determined from ac magnetic susceptibility χ_{ac} . The straight lines are guides to the eyes.

bars in Fig. 6 are a measure of the width of the superconducting transitions, taken to be the 10% and 90% values of the resistance change associated with the transition.

The T_c vs x data for $\text{Pr}(\text{Os}_{1-x}\text{Ru}_x)_4\text{Sb}_{12}$ displayed in Fig. 6 show T_c being suppressed from both ends, culminating in a minimum of $T_c = 0.75\text{ K}$ near $x=0.6$. The plot of $\rho(0\text{ K})$ vs x displayed in the inset of Fig. 4 indicates a variation in disorder due to substitutional effects. The data approximate a parabola with a maximum near $x=0.3$, similar to what is expected for electrical resistivity in disordered alloys, which is a parabola in $\rho(0\text{ K})$ with a maximum at $x=0.5$.^{21,22} In a conventional BCS phonon-mediated superconductor, the reduction of T_c by potential scattering from nonmagnetic solute ions is expected to be small,²³ unless the increase in scattering accompanies a significant change in the electronic structure of the system. While $\text{PrRu}_4\text{Sb}_{12}$ appears to be a conventional BCS superconductor, $\text{PrOs}_4\text{Sb}_{12}$ is quite unconventional, being a heavy fermion superconductor in which the superconducting electron pairing may be mediated by quadrupolar fluctuations. It is therefore unlikely that a simple disorder explanation can account for the behavior of T_c in the $\text{Pr}(\text{Os}_{1-x}\text{Ru}_x)_4\text{Sb}_{12}$ system.

Because the superconducting mechanisms appear to be quite different between $\text{PrOs}_4\text{Sb}_{12}$ and $\text{PrRu}_4\text{Sb}_{12}$, the depression of T_c from both ends as shown in Fig. 6 could be due to a competition between these two types of superconductivity. Indeed, the persistence of superconductivity throughout the series is unusual, as for heavy fermion f -electron superconductors both magnetic and nonmagnetic impurities generally produce relatively rapid depressions of T_c . When the impurity is of an element that would produce an isostructural superconducting compound, the trend is not as clear. For example, the $\text{U}_{1-x}\text{La}_x\text{Pd}_2\text{Al}_3$ system is similar to the $\text{Pr}(\text{Os}_{1-x}\text{Ru}_x)_4\text{Sb}_{12}$ system in that one end member compound, UPd_2Al_3 , is a heavy fermion superconductor, while the other end member compound, LaPd_2Al_3 , is a conventional BCS superconductor. Unlike $\text{Pr}(\text{Os}_{1-x}\text{Ru}_x)_4\text{Sb}_{12}$,

however, superconductivity is destroyed upon substitution on either end of the series.²⁴ This persistence of superconductivity throughout the $\text{Pr}(\text{Os}_{1-x}\text{Ru}_x)_4\text{Sb}_{12}$ system for all values of x is also observed in the $\text{CeCo}_{1-x}\text{Ir}_x\text{In}_5$ series of compounds.²⁵ This system's similarities to $\text{Pr}(\text{Os}_{1-x}\text{Ru}_x)_4\text{Sb}_{12}$ may end there, because both end member compounds (CeCoIn_5 and CeIrIn_5) are heavy fermion superconductors in which the superconductivity is believed to be magnetically mediated and to possess line nodes in the energy gap $\Delta(\mathbf{k})$.²⁶

This nodal energy-gap structure appears to be in contrast with $\text{PrOs}_4\text{Sb}_{12}$, where μSR (Ref. 6) and Sb-NQR (Ref. 7) measurements indicate an isotropic energy gap, a condition which could occur if the superconductivity in $\text{PrOs}_4\text{Sb}_{12}$ was mediated by quadrupolar fluctuations. Tunneling spectroscopy measurements in the superconducting state also indicate that the energy gap of $\text{PrOs}_4\text{Sb}_{12}$ is open over a large part of the Fermi surface, ruling out the presence of line nodes.²⁷ It is generally the case that superconductors with isotropic or nearly isotropic energy gaps are relatively insensitive to the presence of nonmagnetic impurities, with the notable exception of the isotropic p -wave Balian-Werthamer-type superconductivity. Thus, the gradual decrease of T_c , and the presence of superconductivity for all values of x in $\text{Pr}(\text{Os}_{1-x}\text{Ru}_x)_4\text{Sb}_{12}$, provides further evidence for an isotropic energy gap and quadrupolar superconductivity in $\text{PrOs}_4\text{Sb}_{12}$, since $\text{PrRu}_4\text{Sb}_{12}$ also possesses an isotropic superconducting energy gap.¹⁹ The minimum in T_c near $x = 0.6$ could mark the shift from quadrupolar mediated heavy fermion superconductivity to phonon-mediated BCS superconductivity. Specific-heat measurements are in progress, and it will be interesting to see if the heavy fermion state can be correlated with T_c .

On the other hand, several recent experiments indicate the presence of point nodes in the energy gap, most notably thermal-conductivity measurements on $\text{PrOs}_4\text{Sb}_{12}$ in a magnetic field, which have been interpreted in terms of two distinct superconducting phases in the H - T plane, one with two point nodes in $\Delta(\mathbf{k})$ in low fields, and another with six point nodes in $\Delta(\mathbf{k})$ at higher fields.¹¹ In addition, zero-field μSR experiments on $\text{PrOs}_4\text{Sb}_{12}$ have discovered internal magnetic fields in the superconducting state, indicating the breaking of time-reversal symmetry,²⁸ and recent magnetic penetration depth studies also suggest this symmetry breaking as well as the presence of point nodes in the energy gap.²⁹ It is clear that the superconducting state of $\text{PrOs}_4\text{Sb}_{12}$ is not well understood, and the study of how the nature of the superconducting state evolves with Ru substitution could be instrumental in improving this understanding.

B. Crystalline electric field effects

The $\chi_{\text{dc}}(T)$ and $\rho(T)$ data for $\text{Pr}(\text{Os}_{1-x}\text{Ru}_x)_4\text{Sb}_{12}$ were fit to equations including CEF effects, in a manner identical to that reported previously.^{1,15} The CEF equations were derived from the point-charge (i.e., disregarding hybridization effects) Hamiltonian of Lea, Leask, and Wolf (LLW).³⁰ In the LLW formalism, the CEF energy levels are given in terms of the parameters x_{LLW} and W , where x_{LLW} is the ratio of the

fourth- and sixth-order terms of the angular momentum operators in the crystal-field Hamiltonian and W is an overall energy scale factor. It was assumed that the CEF parameter y which controls the tetrahedral T_h crystalline symmetry contribution to the Hamiltonian⁵ was small; thus, the calculations were made for a cubic O_h crystalline symmetry. This assumption was made based on calculations including the T_h terms, which mix the Γ_4 and Γ_5 triplet states into one another. When y is small, the only noticeable change to the physical properties in zero magnetic field is an effect identical to a reduction of the energy-level splitting. Thus, the physical properties induced by a small value of y are identical to those that could be attained by simply changing x_{LLW} and W slightly. When y is large, the mixing of the triplets changes the physical properties drastically. For example, in $\chi(T)$ a Γ_3 - Γ_5 transition manifests itself as a peak, whereas a Γ_3 - Γ_4 transition gives rise to a plateau in $\chi(T)$ at low temperatures. Thus, when the Γ_4 and Γ_5 triplets mix, the shape of the data at low temperatures can change in a dramatic way. In addition, for large enough values of y , a Γ_4 or Γ_5 triplet will be the ground state regardless of the value of x_{LLW} , a condition that is clearly not the case in nonmagnetic $\text{PrOs}_4\text{Sb}_{12}$. Finally, a practical reason for disregarding the addition of terms proportional to y is that this causes the eigenvectors of the LLW Hamiltonian to become dependent on x_{LLW} and W , so fitting the data would become nearly impossible by conventional methods, as the equations for $\chi_{\text{dc}}(T)$ and $\rho(T)$ are derived from transition probabilities that are constant within a given J multiplet. Thus, it was felt that neglecting y was a reasonable approximation, which would only cause small errors in x_{LLW} , W , and the fits described in the remainder of this section. It should be noted that assuming that y is small also implies that the main contribution to the crystalline electric field comes from the simple cubic transition-metal sublattice (Os or Ru), as opposed to the more complicated tetrahedral Sb sublattice.

The $\chi_{\text{dc}}(T)$ data for $x \leq 0.15$ could be reasonably fit with either a Γ_3 or a Γ_1 ground state and a Γ_5 first excited state. As x increases, the magnitude of the peak in χ_{dc} decreases more rapidly than the temperature T_{max} at which the peak occurs. The peak also broadens until it resembles a hump. These changes with x make it unreasonable to fit a Γ_1 - Γ_5 CEF energy-level scheme to the higher x data, since for these data an energy-level scheme with the correct T_{max} makes the peak too sharp, while the correct hump shape results in a T_{max} that is too high. Thus, for the $\text{Pr}(\text{Os}_{1-x}\text{Ru}_x)_4\text{Sb}_{12}$ samples with $x \geq 0.2$, a Γ_3 ground state best approximated the data. An example of a fit with a Γ_3 ground state for $x = 0.6$ is shown in Fig. 7(a). A plot of the splitting between the ground state and the first excited state vs x is shown in Fig. 8, including all reasonable fits of the $\chi_{\text{dc}}(T)$ data.

The $\text{Pr}(\text{Os}_{1-x}\text{Ru}_x)_4\text{Sb}_{12}$ samples with $x \geq 0.6$ all display upturns in $\chi_{\text{dc}}(T)$ at the lowest temperatures [inset (b) in Fig. 2]. If the ground state is a Γ_3 doublet, these upturns could be due to the splitting of the doublet in a small magnetic field H . It would be expected that these upturns would be more noticeable for samples with large x (more Ru than Os), since the CEF contribution to χ_{dc} from the Γ_3 - Γ_5 splitting is much smaller compared to the samples with small x (more Os than

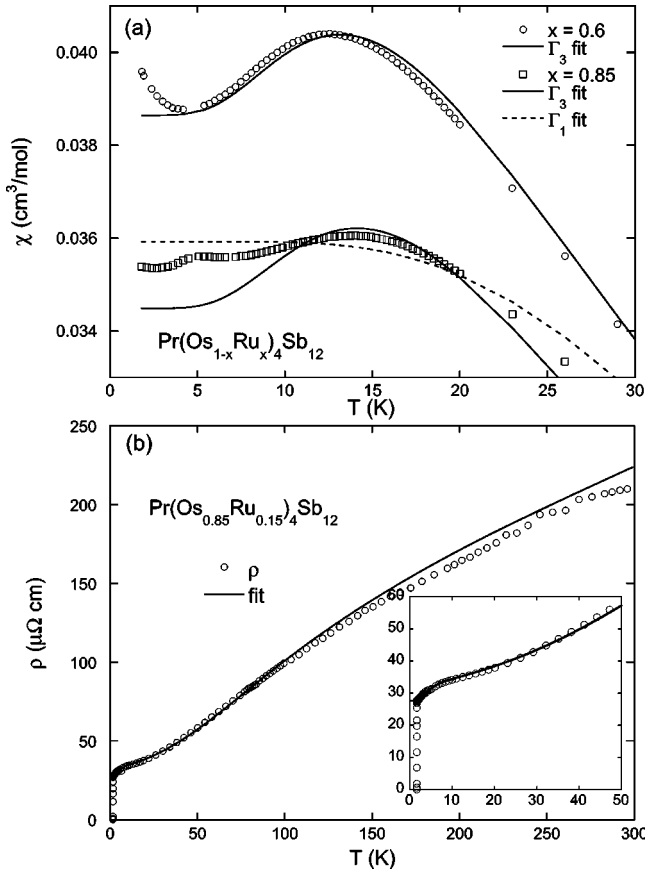


FIG. 7. Examples of CEF fits to the data. (a) dc magnetic susceptibility $\chi_{dc}(T)$ for $x=0.6$ and $x=0.85$ for $\text{Pr}(\text{Os}_{1-x}\text{Ru}_x)_4\text{Sb}_{12}$. The solid lines are fits assuming a Γ_3 doublet ground state and a Γ_5 triplet first excited state, and the dashed line is a fit assuming a Γ_1 singlet ground state and a Γ_4 triplet first excited state. (b) Electrical resistivity $\rho(T)$ for $x=0.15$ between 1 K and 300 K. The fit is for a Γ_3 ground state and a Γ_5 first excited state. Fits with a Γ_1 ground state were qualitatively identical, and so are not shown (see text for details). Inset to (b) $\rho(T)$ for $x=0.15$ between 1 K and 50 K, displaying the low-temperature curvature in greater detail.

Ru). The samples with $x \geq 0.75$, including $\text{PrRu}_4\text{Sb}_{12}$, also display structure in these upturns that appears to be an additional peak near 5 K superimposed on the broad CEF hump, near the temperature of the CEF peak in $\text{PrOs}_4\text{Sb}_{12}$. The smooth progression of both the lattice parameter a and T_c indicates that there is no macroscopic phase separation of $\text{Pr}(\text{Os}_{1-x}\text{Ru}_x)_4\text{Sb}_{12}$ into $\text{PrOs}_4\text{Sb}_{12}$ and $\text{PrRu}_4\text{Sb}_{12}$. However, it is possible that the peaklike structure could be due to inhomogeneous alloying of Os and Ru on an atomic scale, wherein each Pr^{3+} ion sees a distribution of Os or Ru atoms, leading to a variation in the CEF throughout the crystal. Unfortunately, this possibility would be difficult to establish in the current experiments. The low-temperature upturn, especially in $\text{PrRu}_4\text{Sb}_{12}$, could be attributed to either CEF splitting in H or paramagnetic impurities, both of which could produce a low-temperature increase in χ_{dc} .

Takeda *et al.* reported that $\text{PrRu}_4\text{Sb}_{12}$ has a Γ_1 singlet ground state and a Γ_4 triplet first excited state, a CEF configuration that exhibits a plateau in χ_{dc} at low temperatures.¹⁷

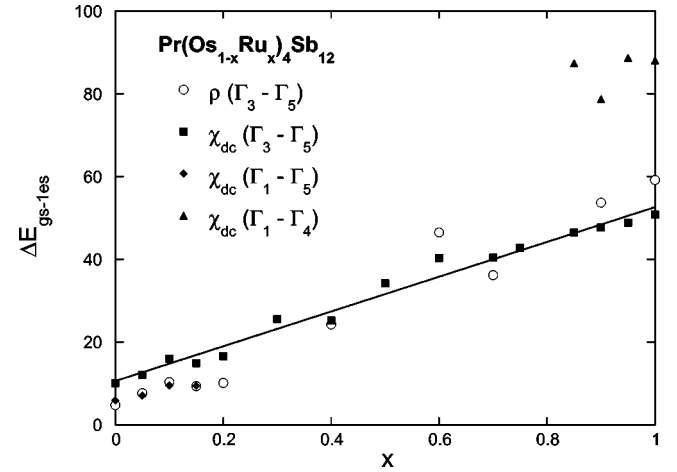


FIG. 8. The splitting between the ground state and first excited state ΔE_{gs-1es} vs Ru concentration x for $\text{Pr}(\text{Os}_{1-x}\text{Ru}_x)_4\text{Sb}_{12}$, calculated from fits of CEF equations to $\chi_{dc}(T)$ and $\rho(T)$, as described in the text. The solid line is a linear fit to ΔE_{gs-1es} for a Γ_3 doublet ground state and a Γ_5 triplet first excited state calculated from the $\chi_{dc}(T)$ data. For $x \leq 0.15$, a CEF energy-level scheme with a Γ_1 singlet ground state and a Γ_5 first excited state also provided a reasonable fit to the $\chi_{dc}(T)$ data, while a Γ_1 ground state with a Γ_4 triplet first excited state was also a possible energy-level scheme for $x \geq 0.85$.

In the current experiment, the $x=0.9$ and $x=1$ samples are the only ones in which a plateau is observed. In addition, while the other samples with $x \geq 0.85$ have their hump maxima reasonably well described by a Γ_3 ground state, the fit predicts a saturation at $T=0$ K that is much lower than is observed in the data. However, the low- T upturn could be responsible for disguising both the maximum in $x=0.9$ and $x=1$ and the low-temperature saturation observed in the other high Ru concentration samples. Accordingly, all the $\text{Pr}(\text{Os}_{1-x}\text{Ru}_x)_4\text{Sb}_{12}$ data with $x \geq 0.85$ were fit assuming both a Γ_3 - Γ_5 CEF energy-level scheme and a Γ_1 - Γ_4 scheme, ignoring the low-temperature upturn; the $x=0.85$ fits are shown in Fig. 7(b). Both fits are represented in the splitting between the ground state and first excited state ΔE_{gs-1es} vs x plot of Fig. 8; the results from all fits are also listed in Table I.

The electrical resistivity $\rho(T)$ of $\text{Pr}(\text{Os}_{1-x}\text{Ru}_x)_4\text{Sb}_{12}$ was fit using a combination of scattering from impurities, the atomic lattice (phonons), and temperature-dependent energy-level populations due to the CEF.¹⁵ The phonon contribution was represented by the measured ρ_{lat} of $\text{LaOs}_4\text{Sb}_{12}$, an isostructural reference compound without f electrons, for all values of x . This procedure was validated by reproducing the results of Abe *et al.*¹⁸ with $\text{LaOs}_4\text{Sb}_{12}$ instead of $\text{LaRu}_4\text{Sb}_{12}$; as expected, the ρ_{lat} data of the two compounds appear to be nearly identical. The CEF contribution to $\rho(T)$ consists of two terms, representing magnetic exchange and aspherical Coulomb scattering, which were assumed to be equally important when fitting the data.¹⁵ Just as it was possible to fit $\rho(T)$ of $\text{PrOs}_4\text{Sb}_{12}$ with either a Γ_3 or a Γ_1 ground state, all of the $\text{Pr}(\text{Os}_{1-x}\text{Ru}_x)_4\text{Sb}_{12}$ data were indifferent to the choice of either ground state. The splitting between the ground state

and the first excited state (always a Γ_5 triplet) was also nearly identical for fits with either ground state for a particular value of x . In the interest of simplicity, for the $\rho(T)$ data, only the splitting between Γ_3 and Γ_5 , ΔE_{3-5} , is shown in Fig. 8. The fit used to calculate ΔE_{3-5} for $x=0.15$ is shown in Fig. 7(b). It is evident that $\rho(H)$ measurements will be required to elucidate the CEF ground state from transport measurements.¹⁵

It is unclear what effect the CEF ground state may have on the superconductivity in $\text{Pr}(\text{Os}_{1-x}\text{Ru}_x)_4\text{Sb}_{12}$. From a physical point of view, it is reasonable that an abrupt change in the ground state would produce an equally abrupt change in the physical properties. However, it is difficult to conceive of a mechanism for this occurrence in the context of the LLW theory, since it is based on the interaction of the atomic lattice with a rare-earth ion. If there is not an abrupt change in the crystal or the electronic structure, which could affect the screening of the CEF, one should not expect an abrupt change in the CEF ground state. It is therefore far more reasonable to consider a constant ground state, with the excited state varying as the Ru substitution changes the spacing of the atoms in the skutterudite lattice. The present data are most consistent with a constant Γ_3 ground state, with the exception of the $x=0.9$ and $x=1$ data. In addition, when x is in the region $0.2 \leq x \leq 0.75$, a Γ_3 - Γ_5 CEF energy-level scheme is the only one which reasonably fits the $\chi_{\text{dc}}(T, x)$ data. On the other hand, the possibility cannot be ruled out that this deep in a substituted system, a CEF analysis in the tradition of LLW may be unreliable due to the distribution of the two substituents (Os and Ru) in the nearest neighbor environment of each Pr^{3+} ion. Finally, the possible effects of hybridization between the f electrons and the conduction electrons were not included in the CEF analysis. These effects are expected to be much stronger for small x , where the

heavy fermion behavior is likely to be strongest. Regardless of the accuracy of the CEF calculations, the steady evolution of the $\chi_{\text{dc}}(T)$ and $\rho(T)$ data does support the gradual increase of the splitting between the ground state and the first excited state. Further experiments as well as theoretical analysis will be necessary to completely reveal the CEF ground state and its relationship to the superconductivity.

V. SUMMARY

The superconducting critical temperature T_c and crystalline electric field (CEF) parameters of single crystals of $\text{Pr}(\text{Os}_{1-x}\text{Ru}_x)_4\text{Sb}_{12}$ have been deduced through measurements of $\chi(T)$ and $\rho(T)$ for $0 \leq x \leq 1$. The superconductivity, which is present for all values of x , exhibits a change in the sign of the slope in $T_c(x)$ near $x=0.6$. It is possible that the crossover from heavy fermion superconductivity that may be mediated by quadrupolar interactions to nearly BCS superconductivity occurs at this ‘‘pseudocritical’’ concentration $x_{pc}=0.6$. The CEF splitting between the ground state and the Γ_5 triplet first excited state increases steadily from $\text{PrOs}_4\text{Sb}_{12}$ to $\text{PrRu}_4\text{Sb}_{12}$, regardless of whether the ground state is a Γ_3 doublet or a Γ_1 singlet. Fits to $\chi_{\text{dc}}(T)$ are most consistent with a Γ_3 ground state throughout the $\text{Pr}(\text{Os}_{1-x}\text{Ru}_x)_4\text{Sb}_{12}$ series, except near $x=1$.

ACKNOWLEDGMENTS

We would like to thank S. K. Kim and D. T. Walker for experimental assistance, and E. D. Bauer for useful discussions. This research was supported by the U.S. Department of Energy Grant No. DE-FG03-86ER-45230, the U.S. National Science Foundation Grant No. DMR-00-72125, and the NEDO International Joint Research Program.

¹E.D. Bauer, N.A. Frederick, P.-C. Ho, V.S. Zapf, and M.B. Maple, Phys. Rev. B **65**, 100506(R) (2002).

²M.B. Maple, P.-C. Ho, V.S. Zapf, N.A. Frederick, E.D. Bauer, W.M. Yuhasz, F.M. Woodward, and J.W. Lynn, J. Phys. Soc. Jpn. **71**, 23 (2002).

³Y. Aoki, T. Namiki, S. Ohsaki, S.R. Saha, H. Sugawara, and H. Sato, J. Phys. Soc. Jpn. **71**, 2098 (2002).

⁴M. Kohgi, K. Iwasa, M. Nakajima, N. Metoki, S. Araki, N. Bernhoeft, J.-M. Mignot, A. Gukasov, H. Sato, Y. Aoki, and H. Sugawara, J. Phys. Soc. Jpn. **72**, 1002 (2003).

⁵K. Takegahara, H. Harima, and A. Yanase, J. Phys. Soc. Jpn. **70**, 1190 (2001).

⁶D.E. MacLaughlin, J.E. Sonier, R.H. Heffner, O.O. Bernal, B.-L. Young, M.S. Rose, G.D. Morris, E.D. Bauer, T.D. Do, and M.B. Maple, Phys. Rev. Lett. **89**, 157001 (2002).

⁷H. Kotegawa, M. Yogi, Y. Imamura, Y. Kawasaki, G.q. Zheng, Y. Kitaoka, S. Ohsaki, H. Sugawara, Y. Aoki, and H. Sato, Phys. Rev. Lett. **90**, 027001 (2003).

⁸M.B. Maple, P.-C. Ho, N.A. Frederick, V.S. Zapf, W.M. Yuhasz, and E.D. Bauer, Acta Phys. Pol. B **34**, 919 (2003).

⁹R. Vollmer, A. Faißt, C. Pfleiderer, H.v. Löhneysen, E.D. Bauer,

P.-C. Ho, V.S. Zapf, and M.B. Maple, Phys. Rev. Lett. **90**, 057001 (2003).

¹⁰N. Oeschler, P. Gegenwart, F. Steglich, N.A. Frederick, E.D. Bauer, and M.B. Maple, Acta Phys. Pol. B **34**, 959 (2003).

¹¹K. Izawa, Y. Nakajima, J. Goryo, Y. Matsuda, S. Osaki, H. Sugawara, H. Sato, P. Thalmeier, and K. Maki, Phys. Rev. Lett. **90**, 117001 (2003).

¹²P.-C. Ho, V.S. Zapf, E.D. Bauer, N.A. Frederick, and M.B. Maple, Int. J. Mod. Phys. B **16**, 3008 (2002).

¹³P.-C. Ho, N.A. Frederick, V.S. Zapf, E.D. Bauer, T.D. Do, M.B. Maple, A.D. Christianson, and A.H. Lacerda, Phys. Rev. B **67**, 180508(R) (2003).

¹⁴N. Oeschler, P. Gegenwart, F. Weickert, I. Zerec, P. Thalmeier, F. Steglich, E. D. Bauer, N. A. Frederick, and M. B. Maple (unpublished).

¹⁵N.A. Frederick and M.B. Maple, J. Phys.: Condens. Matter **15**, 4789 (2003).

¹⁶T. Tayama, T. Sakakibara, K. Kitami, M. Yokoyama, K. Tenya, H. Amitsuka, D. Aoki, Y. Onuki, and Z. Kletowski, J. Phys. Soc. Jpn. **70**, 248 (2001).

¹⁷N. Takeda and M. Ishikawa, J. Phys. Soc. Jpn. **69**, 868 (2000).

- ¹⁸K. Abe, H. Sato, T.D. Matsuda, T. Namiki, H. Sugawara, and Y. Aoki, *J. Phys.: Condens. Matter* **14**, 11 757 (2002).
- ¹⁹M. Yogi, H. Kotegawa, Y. Imamura, G.q. Zheng, Y. Kitaoka, H. Sugawara, and H. Sato, *Phys. Rev. B* **67**, 180501 (2003).
- ²⁰D.J. Braun and W. Jeitschko, *J. Less-Common Met.* **72**, 147 (1980).
- ²¹N. F. Mott and H. Jones, *Theory of the Properties of Metals and Alloys* (Dover, New York, 1936).
- ²²L. Nordheim, *Ann. Phys. (Leipzig)* **9**, 42 (1931).
- ²³P.W. Anderson, *J. Phys. Chem. Solids* **11**, 26 (1959).
- ²⁴V.S. Zapf, R.P. Dickey, E.J. Freeman, C. Sirvent, and M.B. Maple, *Phys. Rev. B* **65**, 024437 (2001).
- ²⁵P.G. Pagliuso, R. Movshovich, A.D. Bianchi, M. Nicklas, N.O. Moreno, J.D. Thompson, M.F. Hundley, J.L. Sarrao, and Z. Fisk, *Physica B* **312-313**, 129 (2002).
- ²⁶R. Movshovich, A. Bianchi, M. Jaime, M.F. Hundley, J.D. Thompson, N. Curro, P.C. Hammel, Z. Fisk, P.G. Pagliuso, and J.L. Sarrao, *Physica B* **312-313**, 7 (2002).
- ²⁷H. Suderow, S. Vieira, J.D. Strand, S. Bud'ko, and P.C. Canfield, cond-mat/0306463 (unpublished).
- ²⁸Y. Aoki, A. Tsuchiya, T. Kanayama, S.R. Saha, H. Sugawara, H. Sato, W. Higemoto, A. Kodo, K. Ohishi, K. Nishiyama, and R. Kadomo, *Phys. Rev. Lett.* **91**, 067003 (2003).
- ²⁹E.E.M. Chia, M.B. Salamon, H. Sugawara, and H. Sato, *Phys. Rev. Lett.* **91**, 247003 (2003).
- ³⁰K.R. Lea, M.J.M. Leask, and W.P. Wolf, *J. Phys. Chem. Solids* **23**, 1381 (1962).